

# RapidLayout: Fast Hard Block Placement of FPGA-optimized Systolic Arrays using Evolutionary Algorithms

Niansong Zhang  
Sun Yat-sen University  
Guangzhou, China  
zhangns@mail2.sysu.edu.cn

Xiang Chen  
Sun Yat-sen University  
Guangzhou, China  
chenxiang@mail.sysu.edu.cn

Nachiket Kapre  
University of Waterloo  
Ontario, Canada  
nachiket@uwaterloo.ca

**Abstract**—Evolutionary algorithms can outperform conventional placement algorithms such as simulated annealing, analytical placement as well as manual placement on metrics such as runtime, wirelength, pipelining cost, and clock frequency when mapping FPGA hard block intensive designs such as systolic arrays on Xilinx UltraScale+ FPGAs. For certain hard-block intensive, systolic array accelerator designs, the commercial-grade Xilinx Vivado CAD tool is unable to provide a legal routing solution without tedious manual placement constraints. Instead, we formulate an automatic FPGA placement algorithm for these hard blocks as a multi-objective optimization problem that targets wirelength squared and maximum bounding box size metrics. We build an end-to-end placement and routing flow called RapidLayout using the Xilinx RapidWright framework. RapidLayout runs 5–6 $\times$  faster than Vivado with manual constraints, and eliminates the weeks long effort to manually generate placement constraints for the hard blocks. We also perform automated post-placement pipelining of the long wires inside each convolution block to target 650 MHz URAM-limited operation. RapidLayout outperforms (1) the simulated annealer in VPR by 33% in runtime, 1.9–2.4 $\times$  in wirelength, and 3–4 $\times$  in bounding box size, while also (2) beating the analytical placer UTPlaceF by 9.3 $\times$  in runtime, 1.8–2.2 $\times$  in wirelength, and 11–14 $\times$  in bounding box size. We employ transfer learning from a base FPGA device to speed-up placement optimization for similar FPGA devices in the UltraScale+ family by 11–14 $\times$  than learning the placements from scratch.

## I. INTRODUCTION

Modern high-end FPGAs provide high compute density with a heterogeneous mixture of millions of classic lookup tables and programmable routing network along with tens of thousands of DSP and RAM hard blocks. These hard blocks offer ASIC-like density and performance for signal processing functions, and on-chip SRAM access. For example, Xilinx UltraScale+ VU11P is equipped with 960 UltraRAM blocks, 4032 Block RAM slices, and 9216 DSP48 blocks capable of operating at 650–891 MHz frequencies which are typically unheard of with LUT-only designs. Furthermore, these hard blocks provide specialized nearest-neighbour interconnect for high-bandwidth, low-latency *cascade* data movement. These features make it particular attractive for building systolic neural network accelerators such as CLP [28], [29], Cascades [27], and Xilinx SuperTile [34], [35].

Exploiting the full capacity of FPGA resources including hard blocks at high clock frequency is challenging. The CLP designs presented in [28], [29] only operate at 100–170 MHz on Virtex-7 FPGAs but leave DSPs unused. The Xilinx SuperTile [34], [35] designs run at 720 MHz, but leaves half the DSPs unused, and also wastes URAM bandwidth by limiting access. The chip-spanning 650 MHz 1920 $\times$ 9 systolic array design for the VU11P FPGA [27] requires 95% or more of the hard block resources but fails routing in commercial-grade Xilinx Vivado run with high effort due to congestion. Manual placement constraints are necessary to enable successful bitstream generation but this requires weeks of painful trial-and-error effort and visual cues in the Vivado floorplanner for correct setup. This effort is needed largely due to irregularity and asymmetry of the columnar DSP and RAM fabric and the complex cascade constraints that must be obeyed for the systolic data movement architecture. Once the constraints are configured, Vivado still needs 5–6 hours of compilation time, making design iteration long and inefficient. Furthermore, to ensure high-frequency operation, it becomes necessary to pipeline long wires in the design. Since timing analysis must be done post-implementation, we end up either suffering the long CAD iteration cycles, or overprovisioning unnecessary pipelining registers to avoid the long design times.

Given this state of affairs with the existing tools, we develop RapidLayout: an alternative, automated, fast placement approach for hard block designs. It is important that such a toolflow address the shortcomings of the manual approach by (1) discovering correct placements quickly without the manual trial-and-error loop through slow Vivado invocations, (2) encoding the complex placement restrictions of the data movement within the systolic architecture in the automated algorithm, (3) providing fast wirelength estimation to permit rapid objective function evaluation of candidate solutions, and (4) exploiting design symmetry and overcoming irregularity of the columnar FPGA hard block architecture. Given this wish list, we used the Xilinx RapidWright framework for our tool.

At its core, the toolflow is organized around the design of a novel evolutionary algorithm formulation for hard block placement on the FPGA through multi-objective optimization of



#### D. Evolutionary Algorithms

There have been several attempts of deploying evolutionary algorithms for FPGA placement with limited success. The earliest one by Venkatraman and Patnaik [32] encodes each two-dimensional block location in a gene, and evaluates the population with a fitness function for critical path and area-efficiency. More recently, P. Jamieson [11], [12] points out GAs for FPGA placement are inferior to annealing mainly due to the weakness of crossover operator, and proposed a clustering technique called supergenes [13] to improve its performance.

In this paper, we design a novel combinational gene representation for FPGA hard block placement, and explore two evolutionary algorithms:

1. **NSGA-II**: Non-Dominated Sorting Genetic Algorithm (NSGA-II [6]) is a two decade-old multi-objective evolutionary algorithm that has grown in popularity today for Deep Reinforcement Learning [18] and Neural Architecture Search [20] applications. NSGA-II addresses multi-objective selection with non-dominated filtering and crowd distance sorting, which allow the algorithm effectively explore the solution space and preserve good candidates.
2. **CMA-ES**: Covariance Matrix Adaptation Evolutionary Strategy (CMA-ES) is a continuous domain optimization algorithm for non-linear, ill-conditioned, black-box problems [10]. CMA-ES models candidate solutions as samplings of a  $n$ -dimensional Gaussian variable with mean  $\mu$  and covariance matrix  $C_\sigma$ . At each evolutionary iteration, the population is generated by sampling from  $\mathbb{R}^n$  with updated mean and covariance matrix. Here, cross-over and mutation become adding Gaussian noise to the samplings, which overcomes the weakness of GA's crossover operator. We use the high-dimensional variant proposed in [26] for fast operation in our placement challenge.

### III. RAPIDLAYOUT

The challenge for mapping FPGA-optimized systolic arrays to the Xilinx UltraScale+ device is the placement of hard blocks to their non-uniform, irregular, columnar locations on the fabric while obeying the cascade data movement constraints. We first present our problem formulation, and then discuss how to embed it into the evolutionary algorithms.

#### A. Problem Formulation

To tackle the placement challenge, we formulate the coarse-grained placement of RAMs and DSP blocks as a constrained multi-objective optimization problem. The placement for rest of the logic *i.e.* lookup tables (LUTs) and flip-flops (FFs) is left to Vivado's placer. The multi-objective optimization goal is formalized as follows.

$$\min \sum_{i,j} ((\Delta x_{i,j} + \Delta y_{i,j}) \cdot w_{i,j})^2 \quad (1)$$

$$\min(\max_k BBoxSize(C_k)) \quad (2)$$

subject to:

$$0 \leq x_i, y_i < XMAX, YMAX \quad (3)$$

$$x_i, y_i \neq x_j, y_j \quad (4)$$

if  $i$  is cascaded after  $j$  in the same column:  $x_i = x_j$

$$y_i = \begin{cases} y_j + 1 & i, j \in \{DSP, URAM\} \\ y_j + 2 & i, j \in \{RAMB\} \end{cases} \quad (5)$$

In the equations above:

- $i \in \{DSP, RAM, URAM\}$  denotes physical a hard block to which a logic block is mapped.
- $C_k$  denotes a convolution unit  $k$  that contains 2 URAMs, 18 DSPs, and 8 BRAMs.
- $\Delta x_{i,j} + \Delta y_{i,j}$  is the Manhattan distance between two physical hard blocks  $i$  and  $j$ .
- $w_{i,j}$  is the weight for wirelength estimation, here we use the number of connections between hard block  $i$  and  $j$ .
- $BBoxSize()$  is the bounding box rectangle size (width + height) containing the hard blocks of a convolution unit  $C_k$ .
- $x_i$  and  $y_i$  denotes the RPM absolute grid co-ordinates of hard block  $i$  that are needed to compute wirelength and bounding box sizes [36].

**Understanding the Objective Function:** We approximate routing congestion performance with squared wirelength (Equation 1) and critical path length with maximum bounding box size (Equation 2). These twin objectives try to reduce pipelining requirements while maximizing clock frequency of operation. While these optimization targets may seem odd, we have observed cases where chasing wirelength<sup>2</sup> alone has misled the optimizer into generating wide bounding boxes for a few stray convolution blocks. In contrast, optimizing for maximum bounding box alone was observed to be extremely unstable and causing convergence problems. Hence, we choose these two objective functions to restrict the spread of programmable fabric routing resources, and reduce the length of critical path between hard blocks and associated control logic fanout.

**Understanding Constraints** The optimizer only needs to obey three constraints. The **region constraint** in Equation 3 restrict the set of legal locations for the hard blocks to a particular repeatable rectangular region of size  $XMAX \times YMAX$  on the FPGA. The **exclusivity constraint** in Equation 4 forces the optimizer to prevent multiple hard block from being assigned to the same physical location. The **cascade constraint** in Equation 5 is the “uphill” connectivity restriction imposed due to the nature of the Xilinx UltraScale+ DSP, BRAM, and URAM cascades. For DSPs and URAMs, it is sufficient to place connected blocks next to each other. For BRAMs, the adjacent block of the same type resides at one block away from the current location. This is because RAMB180 and RAMB181, which are both RAMB18 blocks, are interleaved in the same column.

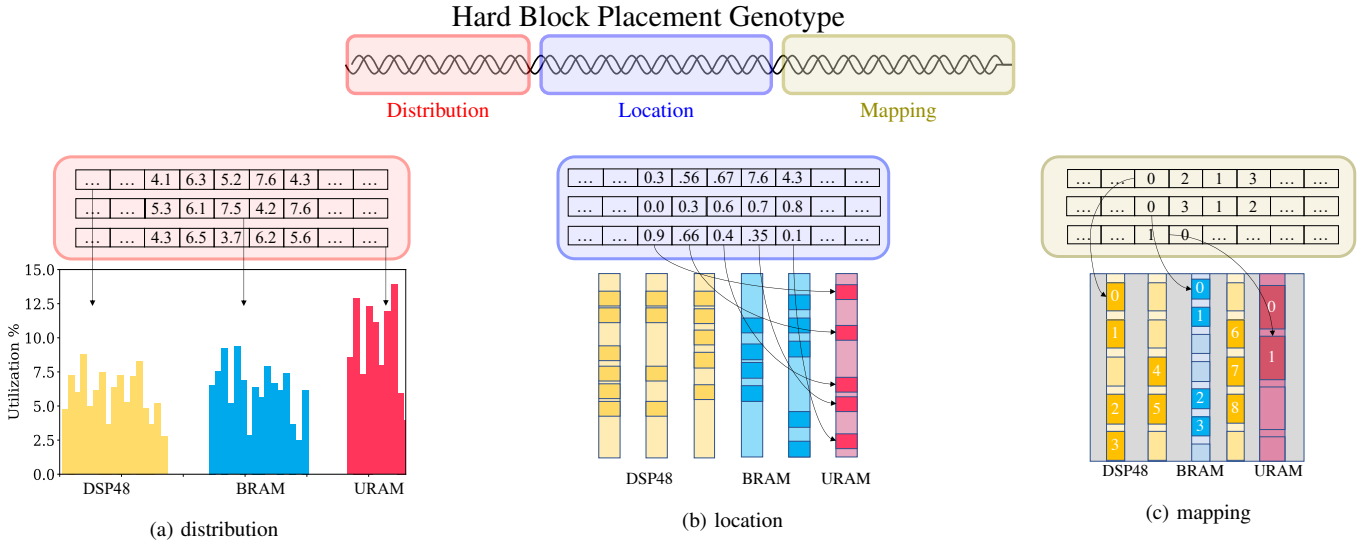


Fig. 2. Our three-tier genotype design for hard block placement. (a) Distribution defines the amount of hard blocks to be placed in each column. (b) Location encodes the relative position of the corresponding hard blocks in its column. (c) Mapping defines the connectivity of hard blocks, i.e., which hard blocks are mapped to one convolution unit. The selected physical hard-block groups are numbered, which corresponds to the mapping genotype.

1) *Genotype Design for Evolutionary Algorithms:* We decompose placement into three sub-problems and encode the candidate solutions with a novel composite genotype design.

1. **Distribution** Since the systolic array accelerator does not perfectly match the hard block resource capacity, we allocate hard blocks across resource columns according to the distribution genotype.
2. **Location** Once we choose the exact number of blocks to place on a given resource column, we assign each block in the column a location according to a value between  $0 \rightarrow 1$ .
3. **Mapping** Finally, we label selected blocks and allocate them to each convolution unit according to the mapping genotype. This is a permutation genotype that optimizes the order of elements without changing its value.

In Figure 2, we visualize the genotype design which consists of the three parts just discussed earlier. During evolution, each part of the genotype is updated and decoded independently, but are evaluated together.

2) *Generality of the Evolutionary Formulation:* The problem formulation and genotype design are motivated by a convolutional systolic array. However, the placement formulation is not limited to any particular hard block design. For example, the computing unit  $C_k$  (Equation 2) can be any hard block design, as long as the number of hard blocks, their connections, and cascade information are provided.

3) *Comparison with Prior Evolutionary Placements:* Our genotype design differs from prior works in three aspects: (1) We provide placement support for heterogeneous hard block types. (2) We encode cascade constraints into the genotype, which eschews extra legalization steps and reduces search space. (3) The three-tier genotype design enables placement transfer learning across devices (Section IV-D).

## B. RapidLayout Design Flow

We now describe the end-to-end RapidLayout design flow:

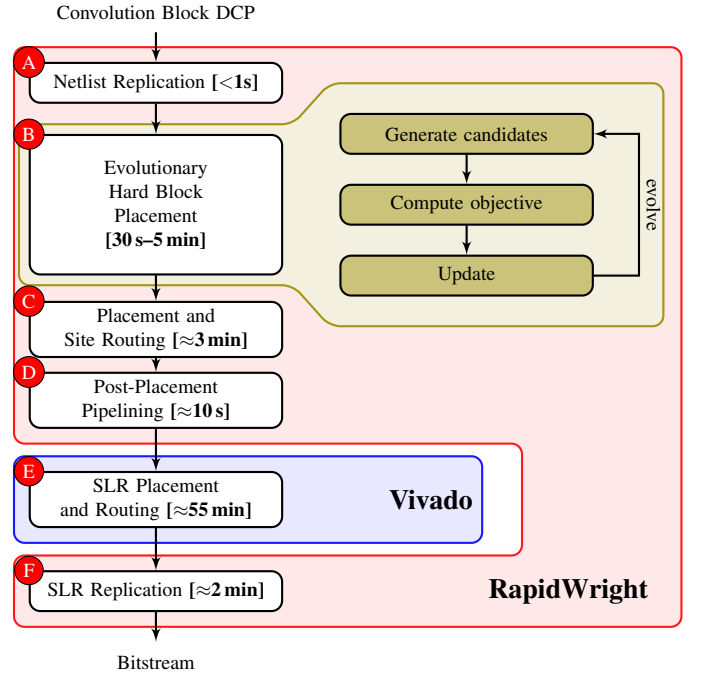


Fig. 3. RapidLayout Design Flow with runtime details for the Xilinx VU11P FPGA along with tool usage information. Bulk of the intelligent exploration is done in RapidWright, and Vivado is only invoked at the end for final placement and routing.

- **Netlist Replication ( $<1s$ )** RapidLayout starts with a synthesized netlist of the convolution unit with direct instantiations of the FPGA hard blocks. The unit design is replicated into the entire logical netlist that maps to the whole Super Logic Region (SLR).
- **Evolutionary Hard Block Placement (30 s–5min)** RapidLayout uses NSGA-II or CMA-ES to generate hard block placement for the minimum repeating rectangular region. Then the rectangular layout is replicated (*copy-paste*) to

produce the placement solution for the entire SLR.

- **Placement and Site Routing ( $\approx 3$  min)** The placement information is embedded in the DCP netlist by placing the hard blocks on the physical blocks called “sites”, followed by “site-routing” to connect intra-site pins.
- **Post-Placement Pipelining ( $\approx 10$  s)** After finalizing placement, we can compute the wirelength for each net in the design and determine the amount of pipelining required for high-frequency operation. This is done post-placement [7], [30], [33] to ensure the correct nets are pipelined and to the right extent. The objective of this step is to aim for 650 MHz URAM-limited operation as dictated by the architectural constraints of the systolic array [27].
- **SLR Placement and Routing ( $\approx 55$  min)** Once the hard blocks are placed and pipelined, we call Vivado to complete LUT/FF placement and routing for the SLR.
- **SLR Replication (1-5 min)** The routed design on the SLR is copied across the entire device using RapidWright APIs to complete the overall implementation.

For VU11P device, RapidLayout accelerates the end-to-end implementation by  $\approx 5$ – $6\times$  when measuring CAD runtime alone ( $\approx$ one hour vs. Vivado’s 5–6 hours). This does not include the weeks of manual tuning effort that is avoided by automatically discovering the best placement for the design.

### C. Example Walkthrough

To illustrate how the different steps help produce the full-chip layout, we walk you through the intermediate stages of the flow. We will inspect three stages of placement, going from a single block layout, to a repeating rectangle layout, and then onto a full-chip layout.

**Single Block layout:** The floorplan of a single convolution block in isolation is shown in Figure 4 where the hard block columns and chosen resources are highlighted. We also highlight the extent of routing requirements between the hard blocks in gray. The locations of the URAM, BRAM, and DSP columns are irregular, which forces a particular arrangement and selection of resource to minimize wirelength and bounding box size. It is clear that a simple *copy-paste* of a single block is not workable due to this irregularity.

**Single Repeating Rectangle Layout:** RapidLayout iteratively bi-partitions one SLR and calculate utilization until the divided section does not fit any unit. Then, the partition scheme with the highest utilization rate is selected to determine the repeating rectangular region. In Figure 5, we show the floorplan for such region. The resource utilization within the rectangle is 100% URAMs, 93.7% DSP48s, and 95.2% BRAMs, which also holds for the entire chip after replication. Our optimizer minimizes overlapping and thus reducing routing congestions to permit high-frequency operation.

**Full-Chip Layout:** The entire chip layout is generated in two steps: (1) First, the rectangular region’s placement is replicated to fill up one SLR (SLR0). The SLR is then pipelined and fully routed. (2) Second, the placement and routing from SLR0’s implementation are replicated across the two other SLRs to fill up the FPGA.

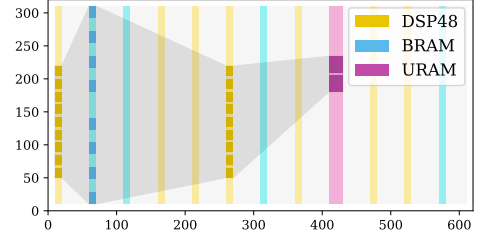


Fig. 4. Floorplan layout visualization of a single convolution block implementation supporting dual  $3\times 3$  kernels to match URAM bandwidth. This is the design shown in Figure 1 earlier. The bounding polygon that encloses all hard blocks and the routing connections is shown in gray.

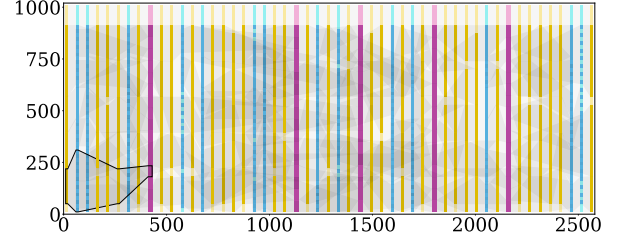


Fig. 5. Floorplan layout visualization of a single repeating rectangular region layout with 80 convolution blocks. The bounding polygon from Figure 4 is also shown here for scale.

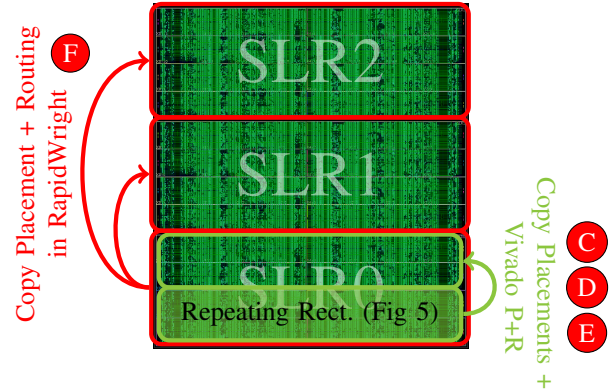


Fig. 6. Full-chip layout for the systolic array accelerator generated from a repeating rectangle of size two clock regions high and the full chip wide. After one replication we span one SLR region. We place and route this with Vivado, export DCP, reimport into RapidWright to clone across SLRs.

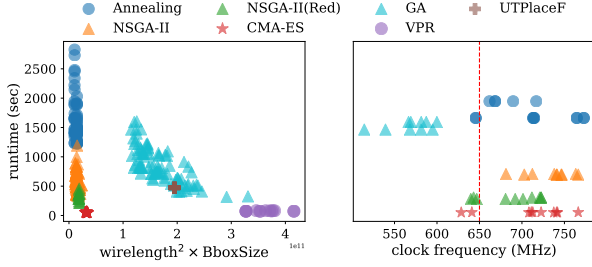
## IV. RESULTS

RapidLayout is implemented in Java to enable seamless integration with RapidWright Java APIs. We use the Java library Opt4J [21] as the optimization framework for NSGA-II, SA and GA. CMA-ES is implemented with Apache Commons Math Optimization Library [25] 3.4 API. We use VPR 7.0 official release [22] and UTPlaceF TCAD version [19] binary for QoR comparison. All placed designs are routed and timed with Vivado Design Suite 2018.3. We run our experiments on an Ubuntu 16.04 LTS machine with Intel Xeon Gold 5115 CPU (10 cores, 20 threads) and 128 GB DDR4 RAM.

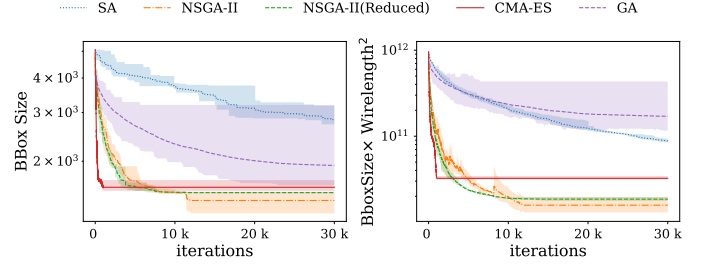
### A. Performance and QoR Comparison

We compare the performance and QoR of evolutionary algorithms against: (1) conventional simulated annealing (SA),





(a) Wirelength, Bounding Box vs. Runtime Comparison



(b) Effect of Convergence on Wirelength, Bounding Box

Fig. 7. Performance, Wirelength, and Bounding Box Comparison: SA, NSGA-II, NSGA-II (Red), and CMA-ES

TABLE I

RUNTIME(AVG), WIRELENGTH(AVG), MAX BBOX(AVG), PIPELINING REGISTERS(MIN), AND FREQUENCY(AVG) FOR ALL METHODS. NSGA-II SHOWS REDUCED GENOTYPE AS WELL. SPEEDUPS AND QOR IMPROVEMENTS WINS BY EVOLUTIONARY ALGORITHMS ALSO REPORTED IN **RED**→NSGA-II AND **GREEN**→CMA-ES FOR EACH COMPETITOR ALGORITHM (SA, GA, UTPLACEF, VPR, MANUAL).

Method	NSGA-II	CMA-ES	SA	GA	VPR	UTPlaceF	Manual
Runtime (secs)	586 (323)	51	1577 (2.7×, 30.8×)	850 (1.5×, 16.7×)	76 (0.13×, 1.5×)	473 (0.8×, 9.3×)	1–2 wks
Wirelength	3.5K (3.5K)	4.4K	3.1K (0.9×, 0.7×)	9.2K (2.6×, 2.1×)	8.5K (2.4×, 1.9×)	7.8K (2.2×, 1.8×)	8.1K (2.3×, 1.8×)
BBox	1183 (1543)	1606	1387 (1.2×, 0.9×)	1908 (1.6×, 1.2×)	4941 (4.1×, 3.1×)	3218 (2.7×, 2.0×)	1785 (1.5×, 1.1×)
Pipeline Reg.	256K (273K)	273K	273K (1.1×, 1×)	323K (1.3×, 1.2×)	-	-	306K (1.2×, 1.1×)
Frequency (MHz)	733 (688)	708	711 (1.03×, 0.99×)	585 (1.3×, 1.2×)	-	-	693 (1.1×, 1.02×)

(2) academic placement tool VPR 7.0, (3) state-of-art analytical placer UTPlaceF, (4) single-objective genetic algorithm (GA) [37], and (5) manual placement design. We exclude RapidWright’s default annealing-based block placer since it does not give feasible placement solution. We run each placement algorithm 50 times with seeded random initialization. Then, we select the top-10 results for each method to route and report clock frequency. While we include VPR and UTPlaceF in the comparisons, they do not support **cascade** constraints (Equation 5). This limits our comparison to an approximate check on solution quality and runtime, and we are unable to directly translate the resulting placement to the FPGA.

In Figure 7a, we plot total runtime and final optimized  $\text{wirelength}^2 \times \text{maximum bounding box size}$  for the different placement algorithms along with Vivado-reported frequency results. We see some clear trends here: (1) NSGA-II is  $\approx 2.7\times$  faster than SA and delivers  $1.2\times$  bounding box improvement, but has  $\approx 12.9\%$  longer wirelength. The average clock frequency of top-10 results is evidently higher than SA as NSGA-II’s performance is more stable. (2) CMA-ES is  $\approx 30\times$  faster than SA. Although the average bounding box size ( $\approx 16\%$  larger) and wirelength ( $\approx 42\%$  larger) are worse than SA’s results, CMA-ES achieves a slightly higher average clock frequency at 711 MHz. (4) An alternate NSGA-II method discussed later in Section IV-B2 with a reduced search space delivers roughly 5 times shorter runtime than SA, with only 2.8% clock frequency degradation, which is still above the URAM-limited 650 MHz maximum operating frequency.

In Figure 7b, we see the convergence rate of the different algorithms when observing bounding box sizes and the combined objective. NSGA-II clearly delivers better QoR for wirelength after 10k iterations, while CMA-ES delivers smaller bounding box sizes within a thousand iterations. Across 50

runs, bounding box optimization shows a much more noisy behavior with the exception of CMA-ES. This makes it (1) tricky to rely solely on bounding box minimization and (2) suggests a preference for CMA-ES for containing critical paths within bounding boxes.

Finally, in Table I, we compare average metric values across the 50 runs of all methods. NSGA-II and CMA-ES deliver superior QoR and runtime against UTPlaceF and VPR, and speeds up runtime by 3–30× against annealing with a minor loss in QoR. Table I also reports the number of registers needed for 650 MHz operation. NSGA-II delivers this with 17k ( $\approx 6\%$ ) less registers against annealing and 50k ( $\approx 16\%$ ) less registers against manual placement. NSGA-II results in Table I are run in 20 threads. Although CMA-ES runs in serial, the runtime is  $\approx 10\times$  faster than NSGA-II with a QoR gap.

### B. Parameter Tuning for Annealing and NSGA-II

In this section, we discuss cooling schedule selection for annealing and optimizations to NSGA-II to explore quality, runtime tradeoffs.

1) *Parameter Tuning for SA*: Cooling schedule determines the final placement quality, but it is highly problem specific. We plot the cooling schedule tuning process in Figure 8, and choose hyperbolic cooling schedule for placement experiments presented in Table I to achieve the best result quality.

2) *NSGA-II Reduced Genotype*: As per the genotype design, distribution and location genotypes take up a large portion of the composite genotype, and they demand special legalization steps. However, for high-utilization designs, distribution and location are less influential since resources are nearly fully utilized. Therefore, we reduce the genotype to mapping only for NSGA-II, and uniformly distribute and stack the hard blocks from bottom to top. As a consequence of this

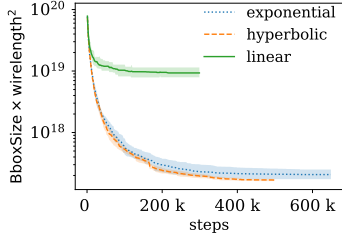


Fig. 8. SA Parameter Tuning. Each type of cooling schedule is experimented with 10 sets of parameter combination. We select hyperbolic cooling schedule with the best parameter combination for annealing placement experiments

trade-off, we observe a  $\approx 1.8\times$  runtime improvement but a  $1.3\times$  larger bounding box size against original NSGA-II. In the convergence plot of Figure 7b, we discover that reduced genotype does not save iteration needed and the bulk of the runtime improvements comes from reduced genotype decoding and legalization work.

### C. Pipelining

Finally, we explore the effect of pipelining stages on different placement algorithms. At each pipelining depth, multiple placements from each algorithm is routed by Vivado to obtain a frequency performance range.

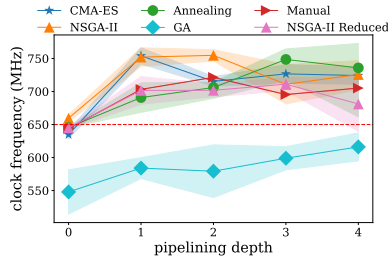


Fig. 9. Effect of post-placement pipelining on clock frequency of the design. NSGA-II delivers 650 MHz without extra pipelining, while CMA-ES, Annealing, and Manual placement requires at least one stage. NSGA-II and CMA-ES achieve 750+ MHz with two stages, while SA requires four stages.

In Figure 9, we show the improvement in frequency as a function of number of pipeline stages inserted along the long wires by RapidLayout. We note that NSGA-II delivers 650 MHz frequency with no pipelining, while others requires at least one stage. Therefore, NSGA-II saves  $\approx 6\%$  registers at pipelining as shown in Table I. NSGA-II wins over manual design at every depth, and CMA-ES exhibits the most stable performance. Systolic array operation at 750+ MHz should be possible with a planned future design refinement of the array design. CMA-ES and NSGA-II can deliver this with only two pipeline stages, while SA requires four stages to achieve the same frequency.

### D. Transfer Learning

RapidLayout is capable of delivering high-quality placement results on devices with different sizes, resource ratio, or column arrangements with transfer learning ability. Transfer learning uses the genotype of an existing placement as a starting seed for initializing the placement search on a new device. We partition Xilinx UltraScale+ family into two groups

TABLE II  
TRANSFER LEARNING PERFORMANCE: VU3P, VU11P AS SEED DEVICES

Device	Design Size (conv units)	Impl.Runtime (mins.)	Frequency (MHz)		Placement Runtime (s)	
			Scratch	Transfer	Scratch	Transfer
<i>xcvu3p</i>	123	46.4	718.9	-	428.3	-
<i>xcvu5p</i>	246	56.9	677.9	660.5	577.9	42.2 (13.7 $\times$ )
<i>xcvu7p</i>	246	55.1	670.2	690.1	578.8	41.9 (13.8 $\times$ )
<i>xcvu9p</i>	369	58.4	684.9	662.3	570.8	42.0 (13.6 $\times$ )
<i>xcvu11p</i>	480	65.2	655.3	-	522.4	-
<i>xcvu13p</i>	640	69.4	653.2	701.3	443.7	38.4 (11.6 $\times$ )

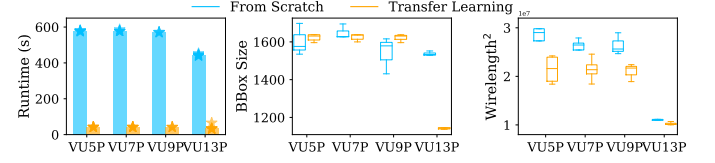


Fig. 10. Runtime and QoR comparison between running from scratch and transfer learning. Transfer learning delivers  $\approx 11\text{--}14\times$  faster runtime,  $0.95\text{--}1.3\times$  bbox size improvement, and  $1.05\text{--}1.17\times$  wirelength improvement

with similar number of hard block columns. We choose VU3P and VU11P as “seed” devices on which RapidLayout generates placement from scratch with NSGA-II. Thereafter, placement results on seed devices are migrated to destination devices in the same group. In Table II and figure 10, we compare placement runtimes with and without transfer learning across a range of FPGA device sizes. We observe that transfer learning accelerates the optimization process by  $11\text{--}14\times$  with a frequency variation between  $-2\%\text{--}+7\%$ . If we observe the total implementation runtime column, we note that SLR replication ensures that the increase in overall runtime (46 mins.  $\rightarrow$  69 mins.,  $1.5\times$ ) with device size is much less than the FPGA capacity increase (123  $\rightarrow$  640,  $5.2\times$ ).

## V. CONCLUSIONS

We present an end-to-end hard block placement workflow for resource intensive systolic array designs on modern heterogeneous FPGAs. We show how to outperform conventional simulated annealing and state-of-art analytical placement with evolutionary algorithms on metrics such as runtime, bounding box size, pipelining cost, and clock period. We formulate the placement of hard blocks as an optimization problem that targets the twin objectives of wirelength and maximum bounding box. RapidLayout delivers an automatic placement-and-routing workflow  $\approx 5\text{--}6\times$  faster than Vivado that eschews manual placement effort. Evolutionary algorithms outperform Simulated Annealing, VPR’s annealer, UTPlaceF analytical placer, and Manual Placement by  $1.5\text{--}30.8\times$  in runtime,  $1.8\text{--}2.4\times$  in wirelength and  $1.1\text{--}4.1\times$  in bounding box sizes. These algorithms also save  $6\text{--}16\%$  pipelining registers to meet the 650 MHz operating frequency constraints. RapidLayout also employs transfer learning to quickly generate placements  $11\text{--}14\times$  faster for similar FPGA devices without requiring a full placement.

## VI. ACKNOWLEDGEMENTS

This work was conducted as part of MITACS Globalink Research Internship in 2019. This work has been supported in part by NSERC and CMC Microsystems. This work was

also supported by University-Industry Collaborative Education Program between Sun Yat-sen University and Diligent Technology. Any opinions, findings, and conclusions or recommendations expressed in this publication are those of the authors and do not necessarily reflect the views of the sponsors

## REFERENCES

- [1] Z. Abuowaimer, D. Maarouf, T. Martin, J. Foxcroft, G. Gréwal, S. Areibi, and A. Vannelli. Gplace3. 0: Routability-driven analytic placer for ultrascale fpga architectures. *ACM Transactions on Design Automation of Electronic Systems (TODAES)*, 23(5):1–33, 2018.
- [2] V. Betz and J. Rose. Vpr: A new packing, placement and routing tool for fpga research. In *International Workshop on Field Programmable Logic and Applications*, pages 213–222. Springer, 1997.
- [3] V. Betz, J. Rose, and A. Marquardt. Architecture and cad for deep-submicron fpgas, chapter appendix b, 1999.
- [4] R. Collier, C. Fobel, L. Richards, and G. Grewal. A formal and empirical analysis of recombination for genetic algorithm-based approaches to the fpga placement problem. In *2012 25th IEEE Canadian Conference on Electrical and Computer Engineering (CCECE)*, pages 1–6. IEEE, 2012.
- [5] J. Dean. The deep learning revolution and its implications for computer architecture and chip design. *arXiv preprint arXiv:1911.05289*, 2019.
- [6] K. Deb, A. Pratap, S. Agarwal, and T. Meyarivan. A fast and elitist multiobjective genetic algorithm: Nsga-ii. *IEEE transactions on evolutionary computation*, 6(2):182–197, 2002.
- [7] K. Eguro and S. Hauck. Simultaneous retiming and placement for pipelined netlists. In *2008 16th International Symposium on Field-Programmable Custom Computing Machines*, pages 139–148, April 2008.
- [8] T. Feist. *Xilinx White Paper: Vivado Design Suite (WP416)*. Xilinx.
- [9] M. Gort and J. H. Anderson. Analytical placement for heterogeneous fpgas. In *22nd international conference on field programmable logic and applications (FPL)*, pages 143–150. IEEE, 2012.
- [10] N. Hansen and A. Ostermeier. Adapting arbitrary normal mutation distributions in evolution strategies: The covariance matrix adaptation. In *Proceedings of IEEE international conference on evolutionary computation*, pages 312–317. IEEE, 1996.
- [11] P. Jamieson. Revisiting genetic algorithms for the fpga placement problem. In *GEM*, pages 16–22, 2010.
- [12] P. Jamieson. Exploring inevitable convergence for a genetic algorithm persistent fpga placer. In *Proceedings of the International Conference on Genetic and Evolutionary Methods (GEM)*, page 1. The Steering Committee of The World Congress in Computer Science, Computer ..., 2011.
- [13] P. Jamieson, F. Gharibian, and L. Shannon. Supergenes in a genetic algorithm for heterogeneous fpga placement. In *2013 IEEE Congress on Evolutionary Computation*, pages 253–260. IEEE, 2013.
- [14] N. P. Jouppi, C. Young, N. Patil, D. Patterson, G. Agrawal, R. Bajwa, S. Bates, S. Bhatia, N. Boden, A. Borchers, R. Boyle, P. Cantin, C. Chao, C. Clark, J. Coriell, M. Daley, M. Dau, J. Dean, B. Gelb, T. V. Ghaemmaghami, R. Gottipati, W. Gulland, R. Hagmann, C. R. Ho, D. Hogberg, J. Hu, R. Hundt, D. Hurt, J. Ibarz, A. Jaffey, A. Jaworski, A. Kaplan, H. Khaitan, D. Killebrew, A. Koch, N. Kumar, S. Lacy, J. Laudon, J. Law, D. Le, C. Leary, Z. Liu, K. Lucke, A. Lundin, G. MacKean, A. Maggiore, M. Mahony, K. Miller, R. Nagarajan, R. Narayanaswami, R. Ni, K. Nix, T. Norrie, M. Omernick, N. Penukonda, A. Phelps, J. Ross, M. Ross, A. Salek, E. Samadiani, C. Severn, G. Sizikov, M. Snellham, J. Souter, D. Steinberg, A. Swing, M. Tan, G. Thorson, B. Tian, H. Toma, E. Tuttle, V. Vasudevan, R. Walter, W. Wang, E. Wilcox, and D. H. Yoon. In-datacenter performance analysis of a tensor processing unit. In *2017 ACM/IEEE 44th Annual International Symposium on Computer Architecture (ISCA)*, pages 1–12, June 2017.
- [15] S. Kirkpatrick, C. D. Gelatt, and M. P. Vecchi. Optimization by simulated annealing. *science*, 220(4598):671–680, 1983.
- [16] Kung. Why systolic architectures? *Computer*, 15(1):37–46, Jan 1982.
- [17] C. Lavin and A. Kaviani. Rapidwright: Enabling custom crafted implementations for fpgas. In *2018 IEEE 26th Annual International Symposium on Field-Programmable Custom Computing Machines (FCCM)*, pages 133–140. IEEE, 2018.
- [18] K. Li, T. Zhang, and R. Wang. Deep reinforcement learning for multi-objective optimization. *arXiv preprint arXiv:1906.02386*, 2019.
- [19] W. Li, S. Dhar, and D. Z. Pan. Utplacef: A routability-driven fpga placer with physical and congestion aware packing. *IEEE Transactions on Computer-Aided Design of Integrated Circuits and Systems*, 37(4):869–882, 2017.
- [20] Z. Lu, I. Whalen, V. Boddeti, Y. Dhebar, K. Deb, E. Goodman, and W. Banzhaf. Nsga-net: neural architecture search using multi-objective genetic algorithm. In *Proceedings of the Genetic and Evolutionary Computation Conference*, pages 419–427. ACM, 2019.
- [21] M. Lukaszewicz, M. Głaś, F. Reimann, and J. Teich. Opt4J - A Modular Framework for Meta-heuristic Optimization. In *Proceedings of the Genetic and Evolutionary Computing Conference (GECCO 2011)*, pages 1723–1730, Dublin, Ireland, 2011.
- [22] J. Luu, J. Goeders, M. Wainberg, A. Somerville, T. Yu, K. Nasartschuk, M. Nasr, S. Wang, T. Liu, N. Ahmed, K. B. Kent, J. Anderson, J. Rose, and V. Betz. Vtr 7.0: Next generation architecture and cad system for fpgas. *ACM Trans. Reconfigurable Technol. Syst.*, 7(2):6:1–6:30, June 2014.
- [23] P. Maidee, C. Ababei, and K. Bazargan. Fast timing-driven partitioning-based placement for island style fpgas. In *Proceedings of the 40th annual design automation conference*, pages 598–603, 2003.
- [24] P. Maidee, C. Ababei, and K. Bazargan. Timing-driven partitioning-based placement for island style fpgas. *IEEE Transactions on Computer-Aided Design of Integrated Circuits and Systems*, 24(3):395–406, 2005.
- [25] A. C. Math. Commons math: The apache commons mathematics library, 2013.
- [26] R. Ros and N. Hansen. A simple modification in cma-es achieving linear time and space complexity. In *International Conference on Parallel Problem Solving from Nature*, pages 296–305. Springer, 2008.
- [27] A. Samajdar, T. Garg, T. Krishna, and N. Kapre. Scaling the cascades: Interconnect-aware fpga implementation of machine learning problems. In *2019 29th International Conference on Field Programmable Logic and Applications (FPL)*, pages 1–8, Sep. 2019.
- [28] Y. Shen, M. Ferdman, and P. Milder. Overcoming resource underutilization in spatial cnn accelerators. In *2016 26th International Conference on Field Programmable Logic and Applications (FPL)*, pages 1–4, Aug 2016.
- [29] Y. Shen, M. Ferdman, and P. Milder. Maximizing cnn accelerator efficiency through resource partitioning. In *Proceedings of the 44th Annual International Symposium on Computer Architecture, ISCA '17*, pages 535–547, New York, NY, USA, 2017. ACM.
- [30] D. P. Singh and S. D. Brown. Integrated retiming and placement for field programmable gate arrays. In *Proceedings of the 2002 ACM/SIGDA Tenth International Symposium on Field-Programmable Gate Arrays, FPGA '02*, page 67–76, New York, NY, USA, 2002. Association for Computing Machinery.
- [31] S. Trimberger and M.-R. Chene. Placement-based partitioning for lookup-table-based fpgas. In *Proceedings 1992 IEEE International Conference on Computer Design: VLSI in Computers & Processors*, pages 91–94. IEEE, 1992.
- [32] R. Venkatraman and L. M. Patnaik. An evolutionary approach to timing driven fpga placement. In *Proceedings of the 10th Great Lakes symposium on VLSI*, pages 81–85, 2000.
- [33] N. Weaver, Y. Markovskiy, Y. Patel, and J. Wawrzynek. Post-placement c-slow retiming for the xilinx virtex fpga. In *Proceedings of the 2003 ACM/SIGDA Eleventh International Symposium on Field Programmable Gate Arrays, FPGA '03*, page 185–194, New York, NY, USA, 2003. Association for Computing Machinery.
- [34] E. Wu, X. Zhang, D. Berman, and I. Cho. A high-throughput reconfigurable processing array for neural networks. In *2017 27th International Conference on Field Programmable Logic and Applications (FPL)*, pages 1–4, Sep. 2017.
- [35] E. Wu, X. Zhang, D. Berman, I. Cho, and J. Thendean. Compute-efficient neural-network acceleration. In *Proceedings of the 2019 ACM/SIGDA International Symposium on Field-Programmable Gate Arrays, FPGA 2019, Seaside, CA, USA, February 24-26, 2019*, pages 191–200, 2019.
- [36] Xilinx. *Vivado Design Suite User Guide, Using Constraints (UG903)*. Xilinx.
- [37] M. Yang, A. Almaini, L. Wang, and P. Wang. An evolutionary approach for symmetrical field programmable gate array placement. In *Research in Microelectronics and Electronics, 2005 PhD*, volume 1, pages 169–172. IEEE, 2005.